


## RESEARCH ARTICLE

# A Compact Ultra-Wideband Power Divider With Enhanced Performance and Error-Tolerant Design Using Microstrip Lines

Mehmet Onur Kok<sup>1</sup>  | Sehabeddin T. İmeci<sup>2</sup> | Alperen Yasa<sup>2,3</sup>

<sup>1</sup>Department of Electrical and Electronic Engineering, Hacı Bektas Veli University, Nevsehir, Turkey | <sup>2</sup>Department of Electric and Electronic Engineering, Fatih Sultan Mehmet Vakıf University, Istanbul, Turkey | <sup>3</sup>Arastatek Elektronik Yazılım A.Ş., Istanbul, Turkey

**Correspondence:** Mehmet Onur Kok (onurkok@nevsehir.edu.tr)

**Received:** 4 August 2025 | **Revised:** 16 November 2025 | **Accepted:** 23 December 2025

**Keywords:** compact WPD | fractional bandwidth | microstrip | power divider | ultra-wideband

## ABSTRACT

This paper presents a compact ultra-wideband (UWB) power divider that uses microstrip lines to achieve stable performance over a wide frequency range. The circuit is designed for wideband operation as well as being easily fabricated using standard FR-4 substrate. Simulation results show that a bandwidth of 5.38 GHz is achieved in the frequency range of 1.6–7.0 GHz and the minimum  $S_{11}$  value is  $-31.78$  dB. The measured transmission coefficients ( $S_{21}$  and  $S_{31}$ ) are in close agreement with the simulated data, both around  $-3.56$  dB, confirming consistent power splitting. The proposed design has been optimized through a detailed parametric study and demonstrates improved isolation and reduced reflection while maintaining simple rectangular geometry. Compared with previous multilayer or high-cost laminate designs, the proposed FR-4-based divider achieves 125% fractional bandwidth and high fabrication tolerance while maintaining a simple geometry suitable for wide-band microwave and communication systems.

## 1 | Introduction

Ultra-wideband (UWB) power dividers are passive RF components that split input signals into multiple outputs and are designed to operate over several gigahertz of bandwidth. They are widely used in multi-band RF front ends, modern communication systems, radar networks, antenna arrays, and measurement setups [1–5]. In wideband applications, parameters such as impedance matching, return loss (RL), isolation, and power balance are critical to achieving high efficiency and accurate signal division. Therefore, the design of wideband power dividers directly affects the overall performance of RF systems.

Several studies have been reported in the literature to improve the performance and bandwidth of UWB power dividers [6–12]. For instance [13], proposed an efficient out-of-phase divider with less than 0.5 dB insertion loss (IL) and a 3.1–10.6 GHz bandwidth. A dual-band Wilkinson divider was developed in [14] using even-mode analysis, operating precisely at 1 and 2 GHz. In [15], bandpass filters employing uniform and step impedance resonators were

introduced to direct different frequency components to separate output ports. A neuro-based miniaturized Wilkinson divider in [16] achieved nearly 50% size reduction while suppressing unwanted bands. The work in [17] introduced a five-resonator design providing high isolation and signal filtering, while [18] demonstrated a tapered-line structure that improved impedance matching and achieved a bandwidth of 2.0–10.2 GHz with 15 dB RL. In [19], a Gysel-type divider offered adjustable power ratios by tuning coupling strength and placing transmission zeros for sharp filtering. A multilayer divider with 85% relative bandwidth and strong common-mode suppression was introduced in [20]. However, its complex three-layer structure resulted in increased fabrication difficulty and height.

In [21], an alternative Wilkinson design was proposed, using multi-mode resonators and parallel-coupled lines instead of conventional  $\lambda/4$  transformers, achieving approximately 78% fractional bandwidth (FBW) but at the cost of added structural complexity. Similarly [22], presented a square-ring multiple-mode resonator divider

with 109% FBW and ~3 dB IL, while [23] utilized open-circuited stubs and coupled lines to realize 97% FBW. A more complex multilayer aperture-backed interdigital structure was introduced in [24], achieving 109% FBW, and [25] demonstrated a broadside-coupled multilayer microstrip divider with 109% FBW and 4.77 dB IL.

Most of the previously reported UWB dividers rely on multilayer configurations or costly high-performance substrates such as RO4003 and RT5880 to achieve wide bandwidth. In contrast, this work highlights a single-layer FR-4 application that maintains UWB performance while offering high fabrication tolerance to dimensional changes, making it highly practical for low-cost mass production. The proposed circuit provides wideband operation from 1.6 to 7.0 GHz (125% FBW), showing good agreement between simulation and measurement and maintaining stable output balance. The complete design process, simulation results, fabrication, measurement, and parametric analysis are presented in the following sections.

## 2 | Theoretical Analysis

Power dividers are essential passive components in RF and microwave engineering and are designed to split an input signal into two or more output signals. They play an important role in communication systems, measurement setups, and antenna networks that require wide-band signal distribution. The operating principles of the proposed design is based on the conventional Wilkinson type divider, which provides equal power distribution and good impedance matching through a  $\lambda/4$  impedance transformer.

The basic theoretical relationships that show the operation of a two-way power divider are summarized below [26].

Calculation of line impedance ( $Z_L$ ):

$$Z_L = \frac{Z_0}{\sqrt{2}}. \quad (2.1)$$

Calculation of line length ( $L$ ):

$$L = \frac{\lambda}{4} * \sqrt{2}. \quad (2.2)$$

Calculation of input power ( $P_{in}$ ):

$$P_{in} = P_{out1} + P_{out2}. \quad (2.3)$$

Calculation of output power ( $P_{out1}$  and  $P_{out2}$ ):

$$P_{out1} = \frac{P_{in}}{2} * \left( \frac{R_2}{(R_1 + R_2)} \right)^2, \quad (2.4)$$

$$P_{out2} = \frac{P_{in}}{2} * \left( \frac{R_1}{(R_1 + R_2)} \right)^2. \quad (2.5)$$

The formulas given use various symbols to represent certain parameters. In this context,  $Z_0$  represents the characteristic impedance of the transmission lines.  $R_L$  is used to indicate the load resistance, which represents the resistance connected to the output ports.  $P_{in}$  indicates the input power, which is the power supplied to the system. Additionally,  $P_{out1}$  and  $P_{out2}$  represent the output powers at Port 1 and Port 2, respectively, indicating the power distributed to these respective ports.

The theoretical  $\lambda/4$  transformer confirms impedance matching between the input and output ports, while the resistive network provides isolation and suppresses reflections. In the proposed UWB configuration, these relationships were used as initial design constraints, and further parametric optimization in Sonnet software adjusted the geometry to maintain low reflection and equal output levels over the 1.6–7.0 GHz band. The combination of analytical design and EM-based optimization provides wide-band load matching and stable amplitude balance.

## 3 | Design and Analysis of the Equal Power Divider

During the initial design phase, each side of the structure was symmetrical by removing various sections. The etched areas between the two output ports were then combined to improve isolation and reduce reflections. When these previously disconnected sections were directly connected, simulation results showed a significant improvement in the overall amplitude response. After the connection was completed, impedance matching was performed at the two output ports to make sure equal power division.

It was observed that long and narrow microstrip sections obstructed current flow at certain frequencies and cause unwanted reflections. Therefore, most of these long strips were removed to reduce  $S_{11}$  and increase the stability of  $S_{21}$  and  $S_{31}$

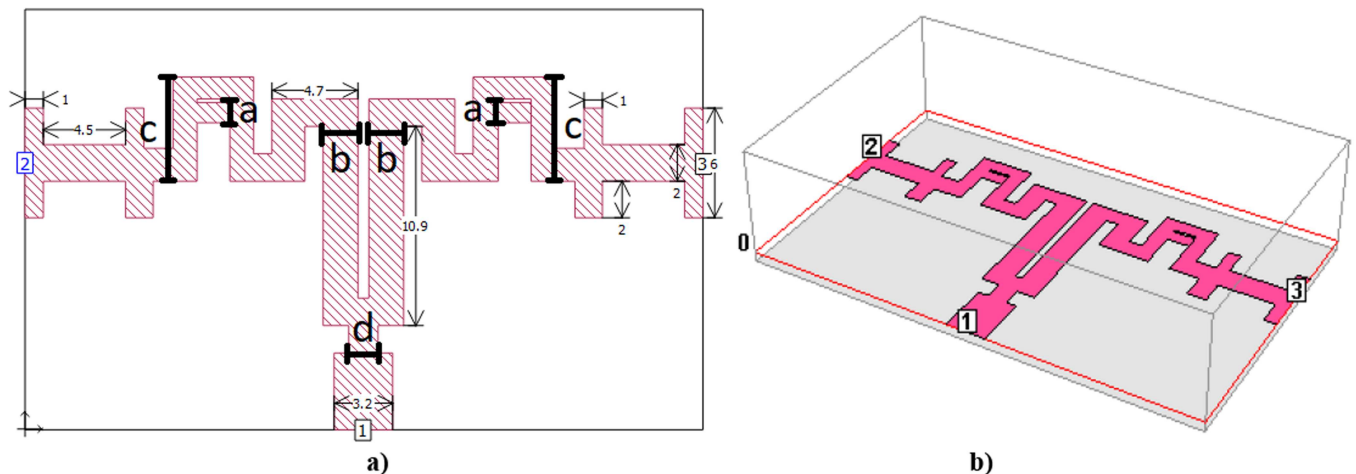


**FIGURE 1** | Proposed design layout. (a) Parametric dimensions (b) 3D view.

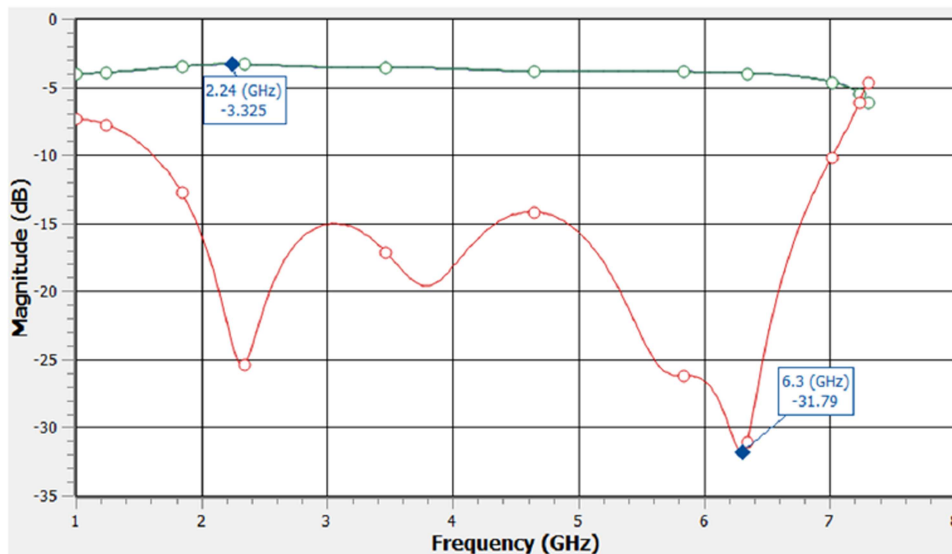


**FIGURE 2** | Simulated result of S-parameters of the proposed power divider.

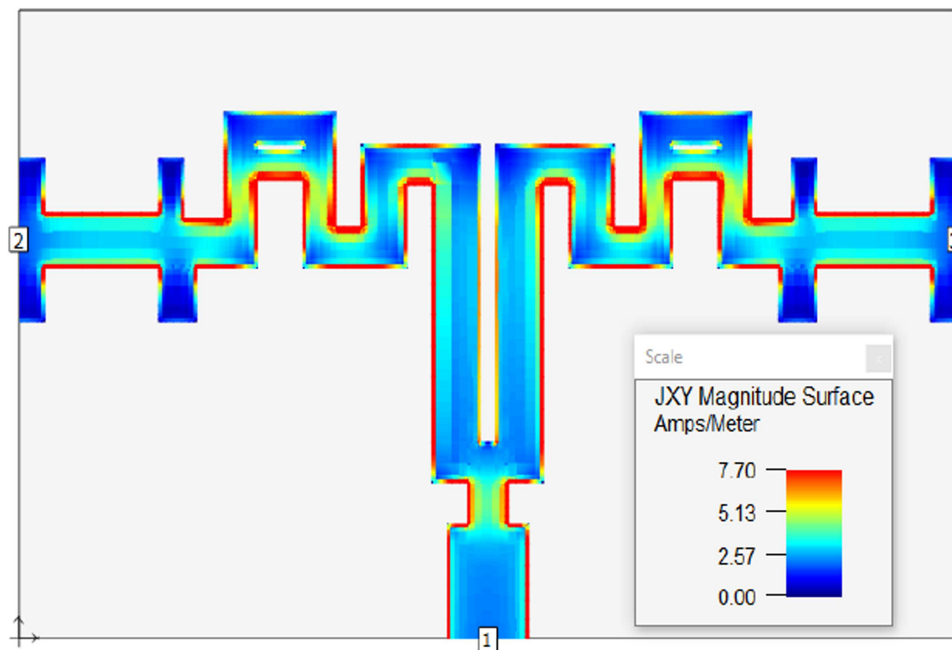


**FIGURE 3** | Current distribution at 1.84 GHz.

by approximately  $-3.0$  dB across the operating band. This optimization improved both bandwidth uniformity and power balance between the output ports.

Figure 1a shows the top view layout of the proposed power divider with key geometric parameters labeled as a, b, c, and d. These parameters were determined to have the most significant impact on the device performance and manufacturing accuracy. They were selected for the parametric analysis which will be presented later in the measurement and tolerance study section. Figure 1b shows the port numbering: Port 1 is the input, while Ports 2 and 3 correspond to the output ports that transmit the divided signals.

The simulated S-parameters of the proposed divider are presented in Figure 2. As can be seen from the figure, the design provides a wide and stable operating bandwidth suitable for a various RF and microwave applications. The proposed power

divider operates effectively between 1.62 and 7.0 GHz and provides a bandwidth of 5.38 GHz. This performance represents a significant improvement over many conventional power dividers, which typically have narrower bandwidths and are less suitable for wide-band signal processing.

To further analyze the electromagnetic behavior, current distribution simulations were performed using the Sonnet software at selected frequencies. These analyses provided insight into how the proposed geometry supports broadband operation and uniform field distribution. Figure 3 illustrates the current distribution at 1.84 GHz, where different colors indicate varying current densities along the transmission lines. The results confirm that the optimized geometry ensures efficient current flow and uniform power distribution between the output ports, validating the effectiveness of the structural modifications.

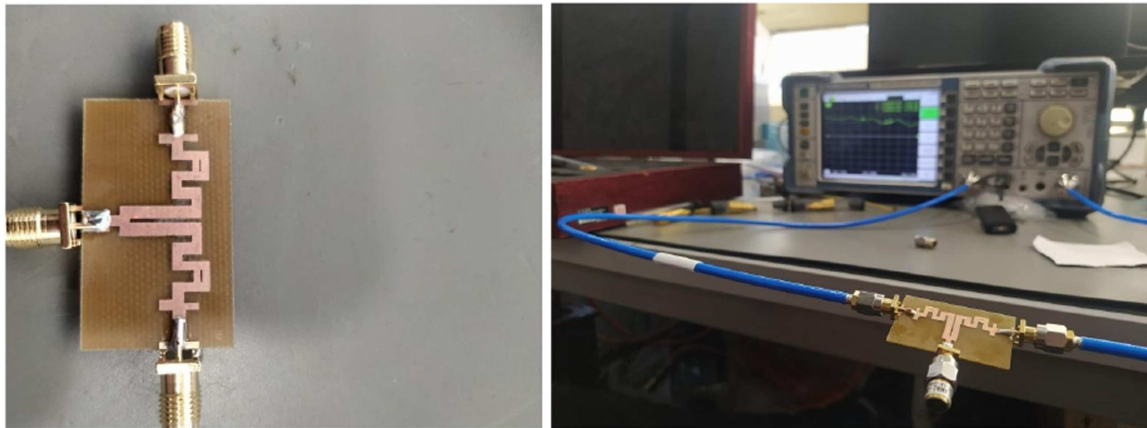


FIGURE 4 | Fabricated power divider and measurement setup.

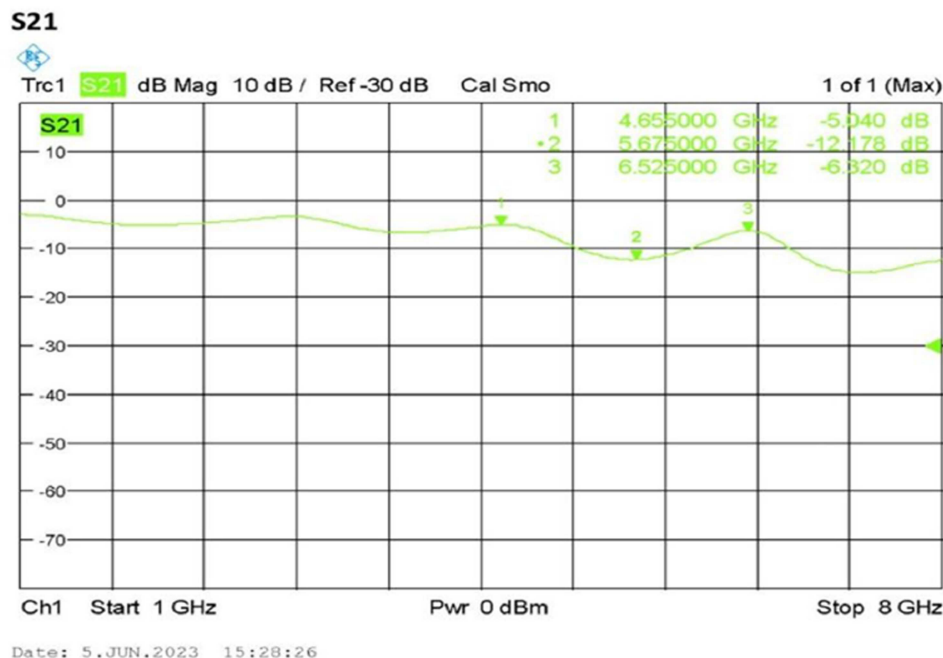


FIGURE 5 | Measurement results of S-parameters.

#### 4 | Measurement Results and Parametric Study

The proposed divider was fabricated on a double-sided copper-clad FR-4 laminate with a thickness of 1 mm. FR-4 was chosen because it is widely used in practical RF and microwave circuits due to its low cost and widespread availability. The circuit was fabricated using a high-precision LPKF milling machine, that precisely removed unwanted copper areas according to the design layout. The design file was transferred as a Gerber file to the milling machine and the layout pattern was precisely milled to form the microstrip structure. After the milling process, the fabricated circuit was carefully separated from the main FR-4 panel.

During assembly, the SMA connectors were soldered to the ports. The upper ground pins of the SMA connectors were shorted to prevent possible short circuits between the ground and signal lines. Since output ports were located near the circuit edges, the connectors were connected slightly away from

boundaries to maintain mechanical clearance and minimize parasitic effects. The fabricated prototype and the measurement setup are shown in Figure 4. The image was taken prior to the experimental analysis.

The measured S-parameters of the fabricated prototype are presented in Figure 5. The measured S<sub>21</sub> shows a similar trend to the simulated results, indicating that the design performs as expected. The small difference observed between simulation and measurement is mainly due to the dielectric and conductive losses of the FR-4 substrate. This substrate is known to have relatively high loss tangent at microwave frequencies. However, the divider maintains its satisfactory performance over the entire operating range.

To evaluate the effect of fabrication tolerances, parametric analysis was performed by varying four critical geometrical parameters, denoted as a, b, c, and d. Each parameter was adjusted within practical limits to observe its effect on bandwidth and magnitude

**TABLE 1** | Effect of the dimension a.

Dimension (mm)	Frequency range (GHz)	Magnitude (dB)	Bandwidth (GHz)
1.1 mm	1.62–7.0	3.66–4.63	5.42
1.3 mm	1.64–7.04	3.66–4.65	5.4
0.9 mm	1.62–7.0	3.65–4.62	5.38
0.7 mm	1.58–6.94	3.64–4.62	5.36
0.5 mm	1.6–6.94	3.65–4.6	5.34

**TABLE 2** | Effect of the dimension b.

Dimension (mm)	Frequency range (GHz)	Magnitude (dB)	Bandwidth (GHz)
2.0 mm	1.6–7.0	3.63–4.64	5.4
1.9 mm	1.62–7.02	3.66–4.63	5.4
1.8 mm	1.64–7.02	3.65–4.64	5.38
1.7 mm	1.62–7.06	3.65–4.64	5.44
1.6 mm	1.6–7.04	3.65–4.65	5.44

**TABLE 3** | Effect of the dimension c.

Dimension (mm)	Frequency range (GHz)	Magnitude (dB)	Bandwidth (GHz)
5.9 mm	1.6–7.08	3.65–4.66	5.48
5.8 mm	1.6–7.06	3.67–4.67	5.46
5.7 mm	1.62–7.02	3.66–4.63	5.4
5.6 mm	1.64–7.0	3.65–4.61	5.36
5.9 mm	1.64–6.98	3.66–4.63	5.34

**TABLE 4** | Effect of the dimension d.

Dimension (mm)	Frequency range (GHz)	Magnitude (dB)	Bandwidth (GHz)
1.2 mm	1.64–6.88	3.67–4.62	5.24
1.4 mm	1.64–6.96	3.65–4.64	5.32
1.6 mm	1.62–7.02	3.66–4.63	5.4
1.8 mm	1.62–7.08	3.65–4.66	5.46
2.0 mm	1.62–7.12	3.63–4.66	5.5

Note: The results show that the bandwidth remains approximately constant (5.3–5.5 GHz) even with small geometric changes. This confirms that the design is tolerant to typical manufacturing deviations. This characteristic makes it suitable for low-cost PCB production without requiring sub-millimeter fabrication precision.

**TABLE 5** | Comparison between the proposed design and selected studies.

Refs.	Bandwidth (GHz)	FBW (%)	RL (dB)	IL (dB)	Dimensions (mm)	Substrate	Topology
[16]	1–3.5	111	> 10	> 4	14.2 × 16.3	RT5880	Filtering-type
[22]	3.1–10.6	109	> 10	~3	20 × 30	RO4003B	Multimode
[23]	3.5–10.1	97	> 10	~3	n/a × 35	RT6010	Single layer
[24]	3.1–10.6	109	> 10	~3	20 × n/a	RT5880	Multilayer
[25]	3.1–10.6	109	> 17	4.77	20 × 30	RO4003C	Multilayer
This work	1.6–7	125	> 15	3.5	23 × 37	FR4	Single layer

response. The simulated results are summarized in Tables 1–4. These results demonstrate the robustness and manufacturability of the design. Moderate parameter variations cause only minor changes in the bandwidth and IL.

Table 5 compares the proposed design with previously reported UWB dividers in terms of bandwidth, FBW, RL, IL, physical dimensions, substrate, and topology. The proposed divider achieves the widest FBW (125%) among comparable single-

layer microstrip structures, with RL better than 15 dB and IL around 3.5 dB. The compact size (23 × 37 mm) and low-cost FR-4 substrate further highlight its practical advantages over complex or multilayer designs. As seen in Table 5, the proposed design outperforms previous single-layer configurations in both bandwidth and manufacturability, while maintaining compact dimensions. Its high FBW, good RL, and consistent power balance make it a strong candidate for cost-sensitive RF and microwave applications such as broadband communication and measurement systems.

## 5 | Conclusion

In this study, a compact UWB power divider is presented that combines several advantageous features such as reduced physical size, easy fabrication, and high tolerance to manufacturing errors. Implemented on a single-layer FR-4 substrate, the design provides 125% FBW from 1.6 to 7.0 GHz while maintaining approximately 3.5 dB IL and better than 15 dB RL across the band. The parametric study shows that small dimensional variations have minimal effect on performance. This confirms the design's robustness and suitability for low-cost mass production. Simulation and measurement results show good agreement. This validates the accuracy of the electromagnetic modeling and confirms stable power division over the entire frequency range. Compared with previously reported designs, the proposed design achieves a wider bandwidth and improved manufacturability using a simple single-layer layout without utilizing multilayer or high-cost laminates. With these characteristics, the proposed UWB power divider represents a practical and efficient solution for broadband applications such as cellular networks, Wi-Fi and WLAN networks, radar front ends, antenna feed networks, and satellite communication links.

### Acknowledgments

We would like to thank SONNET Software [27] for licensing the electromagnetic simulation tool for Fatih Sultan Mehmet Vakif University, and our universities research center BETAM for the fabrication and PROFEN A.Ş. for the measurements.

### Funding

The authors received no specific funding for this work.

### Ethics Statement

This article does not contain any studies involving humans and animals performed by any of the authors.

### Conflicts of Interest

The authors declare no conflicts of interest.

### Data Availability Statement

Data sharing not applicable to this article as no datasets were generated or analysed during the current study. The data that support the findings of this study are available from the author upon reasonable request.

## References

1. G. Moloudian, S. Soltani, S. Bahrami, J. L. Buckley, B. O'Flynn, and A. Lalbakhsh, "Design and Fabrication of a Wilkinson Power Divider With Harmonic Suppression for LTE and GSM Applications," *Scientific Reports* 13, no. 1 (2023): 4246.
2. Ş. T. İmeci, B. Tütüncü, and L. Herceg, "Performance-Enhanced S-Shaped Slotted Patch Antenna for X Band/Ku Band Applications," *Wireless Personal Communications* 129, no. 2 (2023): 1069–1082.
3. S. A. M. Osman, M. S. El-Gendy, H. M. S. Elhennawy, and E. A. Abdallah, "A Miniaturized Wideband Wilkinson Power Divider for IoT Sub-GHz Applications," *Progress In Electromagnetics Research M* 112 (2022): 243–253.
4. M. A. Imani, F. Shama, and G. H. Roshani, "Miniaturized Wilkinson Power Divider With Suppressed Harmonics," *Microwave and Optical Technology Letters* 62, no. 4 (2020): 1526–1532.
5. S. Roshani and S. Roshani, "Design of a Compact LPF and a Miniaturized Wilkinson Power Divider Using Aperiodic Stubs With Harmonic Suppression for Wireless Applications," *Wireless Networks* 26, no. 2 (2020): 1493–1501.
6. S. C. Sivaprakash, K. Monika, and A. Sivanantha Raja, "Wide Band Folded Coupled Line Power Divider Using Metamaterial for Mobile Application," *Wireless Personal Communications* 125, no. 1 (2022): 685–697.
7. A. F. Elshafey, E. K. AbuSaif, and M. A. Abdalla, "A Wideband High-Power Ridge Gap Waveguide Power Divider for High-Power Division Sub-Systems Applications," *IETE Journal of Research* 69, no. 2 (2023): 960–966.
8. Z. Shaterian and A. Karami Horestani, "Ultra-Wideband Multi-Section Wilkinson Power Divider," *Microwave and Optical Technology Letters* 63, no. 1 (2021): 75–81.
9. M. Y. İmeci, B. Tütüncü, and Ş. T. İmeci, "A 3-dB 90 Degrees Microstrip Hybrid Directional Coupler at 2.27 GHz," *AEU-International Journal of Electronics and Communications* 163 (2023): 154606.
10. A. R. Moznebi, K. Afrooz, and M. Danaeian, "High-Performance Filtering Power Divider Based on Air-Filled Substrate Integrated Waveguide Technology," *ETRI Journal* 45, no. 2 (2023): 338–345.
11. J. H. Park, S. J. Park, and M. Q. Lee, "Quadrature Wilkinson Power Divider Using Cross-Type Short-Circuited Shunt Stub for Good Amplitude and Phase Balance," *AEU-International Journal of Electronics and Communications* 170 (2023): 154783.
12. W. Wang, Y. Zheng, and Q. Cao, "A Four-Way Broadband Filtering Power Divider With Improved Matching Network for X-Band Application," *Microwave and Optical Technology Letters* 61, no. 9 (2019): 2155–2160.
13. M. E. Bialkowski and A. M. Abbosh, "Design of a Compact UWB Out-of-Phase Power Divider," *IEEE Microwave and Wireless Components Letters* 17, no. 4 (2007): 289–291.
14. K. K. M. Cheng and C. Law, "A Novel Approach to the Design and Implementation of Dual-Band Power Divider," *IEEE Transactions on Microwave Theory and Techniques* 56, no. 2 (2008): 487–492.
15. H. A. Hussein, Y. S. Mezaal, and B. M. Alameri, "Miniaturized Microstrip Diplexer Based on FR4 Substrate for Wireless Communications," *Elektronika Ir Elektrotehnika* 27, no. 5 (2021): 34–40.
16. M. Jamshidi, A. Lalbakhsh, S. Lotfi, H. Siahkamari, B. Mohamadzade, and J. Jalilian, "A Neuro-Based Approach to Designing a Wilkinson Power Divider," *International Journal of RF and Microwave Computer-Aided Engineering* 30, no. 3 (2020): e22091.
17. X. Y. Zhang, K. X. Wang, and B. J. Hu, "Compact Filtering Power Divider With Enhanced Second-Harmonic Suppression," *IEEE Microwave and Wireless Components Letters* 23, no. 9 (2013): 483–485.
18. C. T. Chiang and B. K. Chung, "Ultra-Wideband Power Divider Using Tapered Line," *Progress in Electromagnetics Research* 106 (2010): 61–73.

19. K. X. Wang, X. Y. Zhang, and B. J. Hu, "Gysel Power Divider With Arbitrary Power Ratios and Filtering Responses Using Coupling Structure," *IEEE Transactions on Microwave Theory and Techniques* 62, no. 3 (2014): 431–440.
20. J. Shi, J. Wang, K. Xu, J. X. Chen, and W. Liu, "A Balanced-to-Balanced Power Divider With Wide Bandwidth," *IEEE Microwave and Wireless Components Letters* 25, no. 9 (2015): 573–575.
21. Y. Liu, L. Zhu, and S. Sun, "Proposal and Design of a Power Divider With Wideband Power Division and Port-to-Port Isolation: A New Topology," *IEEE Transactions on Microwave Theory and Techniques* 68, no. 4 (2020): 1431–1438.
22. J. Y. Wu, M. Du, H. Peng, X. Wang, and Y. Ling, "A New Printed Microstrip UWB Power Divider With Notched Band," *Progress in Electromagnetics Research C* 62 (2016): 71–76.
23. S. W. Wong and L. Zhu, "Ultra-Wideband Power Divider With Good in-Band Splitting and Isolation Performances," *IEEE Microwave and Wireless Components Letters* 18, no. 8 (2008): 518–520.
24. W. Q. Liu, F. Wei, C. H. Pang, and X. W. Shi, "Design of a Compact Ultra-Wideband Power Divider." In *2012 International Conference on Microwave and Millimeter Wave Technology (ICMMT (IEEE, 2012)*, 2, 1–3.
25. A. M. Abbosh, "A Compact UWB Three-Way Power Divider," *IEEE Microwave and Wireless Components Letters* 17, no. 8 (2007): 598–600.
26. D. M. Pozar (2012). *Microwave Engineering*. Fourth Editions, University of Massachusetts at Amherst, John Wiley & Sons, Inc, 26–30.
27. Sonnet Suites, [www.sonnetsoftware.com](http://www.sonnetsoftware.com), Ver. 18.56, Syracuse, New York.